

A UNITED STATES
DEPARTMENT OF
COMMERCE
PUBLICATION

TELECOMMUNICATIONS

Research Report

U.S. DEPARTMENT OF COMMERCE
OFFICE OF TELECOMMUNICATIONS
Institute for Telecommunication Sciences

World Maps of Atmospheric Radio Noise in Universal Time by Numerical Mapping

DONALD H. ZACHARISEN

WILLIAM B. JONES

OFFICE OF TELECOMMUNICATIONS

The Department of Commerce, under the 1970 Executive Order No. 11556, has been given the responsibility of supporting the Government in general and the Office of Telecommunications Policy in particular in the field of telecommunications analysis. The Department of Commerce, in response to these added duties, instituted the Office of Telecommunications as a primary operating unit to meet the demands of telecommunications in the areas of economic, sociological and regulatory research and advice. The Office consists of three units as follows:

Frequency Management/Support Division: Provides centralized technical and administrative support for coordination of Federal frequency uses and assignments, and such other services and administrative functions, including the maintenance of necessary files and data bases, responsive to the needs of the Director of the Office of Telecommunications Policy (OTP) in the Executive Office of the President, in the performance of his responsibilities for the management of the radio spectrum.

Telecommunications Analysis Division: Conducts technical and economic research and analysis of a longer term, continuing nature to provide information and alternatives for the resolution of policy questions, including studies leading to the more efficient allocation and utilization of telecommunication resources; provides forecasts of technological developments affecting telecommunications and estimates their significance; provides advisory services in telecommunications to agencies of Federal, State and local governments; and performs such other analysis as is required to support OTP.

Institute for Telecommunication Sciences: The Institute for Telecommunication Sciences (ITS), as a major arm of the Office of Telecommunications, is the central Federal agency for research on the transmission of radio waves. As such, ITS has the responsibility to:

(a) Acquire, analyze and disseminate data and perform research in general on the description and prediction of electromagnetic wave propagation, and on the nature of electromagnetic noise and interference, and on methods for the more efficient use of the electromagnetic spectrum for telecommunication purposes;

(b) Prepare and issue predictions of electromagnetic wave propagation conditions and warnings of disturbances in those conditions;

(c) Conduct research and analysis on radio systems characteristics, and operating techniques affecting the utilization of the radio spectrum in coordination with specialized, related research and analysis performed by other Federal agencies in their areas of responsibility;

(d) Conduct research and analysis in the general field of telecommunication sciences in support of other Government agencies as required; and

(e) Develop methods of measurement of system performance and standards of practice for telecommunication systems.

This Telecommunications Research Report series is the primary vehicle for early or detailed dissemination of results of research and analysis projects.



U.S. DEPARTMENT OF COMMERCE

Maurice H. Stans, Secretary

OFFICE OF TELECOMMUNICATIONS

Armig G. Kandoian, Director

INSTITUTE FOR TELECOMMUNICATION SCIENCES

Richard C. Kirby, Director

OT/ITS RESEARCH REPORT 2

World Maps of Atmospheric Radio Noise in Universal Time by Numerical Mapping

DONALD H. ZACHARISEN

WILLIAM B. JONES

This work was supported in part by
STRATCOM under contract SCC-413-69

INSTITUTE FOR TELECOMMUNICATION SCIENCES
BOULDER, COLORADO

October 1970

For sale by the Superintendent of Documents, U. S. Government Printing Office, Washington, D. C. 20402

Price 40 cents

TABLE OF CONTENTS

	Page
ABSTRACT	1
1 INTRODUCTION	1
2 CONVERSION OF DATA FROM LOCAL TIME TO UNIVERSAL TIME	4
3 FOURIER ANALYSIS OF THE LONGITUDINAL VARIATION FOR A FIXED LATITUDE	5
4 ANALYSIS OF LATITUDINAL VARIATION OF FOURIER COEFFICIENTS	8
5 FOURIER ANALYSIS OF DIURNAL VARIATION WITHIN A THREE-MONTH PERIOD	13
6 THE MAPPING RESIDUALS	15
7 WORLD MAPS OF THE 1MHZ ATMOSPHERIC NOISE IN UNIVERSAL TIME	18
8 CONCLUSIONS	27
9 REFERENCES	29
APPENDIX A	31

WORLD MAPS
OF ATMOSPHERIC RADIO NOISE IN UNIVERSAL TIME
BY NUMERICAL MAPPING

D. H. Zacharisen and William B. Jones

ABSTRACT

Worldwide atmospheric noise at 1 MHz, as presented in CCIR Report 322 (1963), has been numerically mapped in universal time. The mapping technique and representative contour maps for January and July, are presented. Fourier analyses were performed separately on the periodic functions that represent the longitudinal and diurnal variations of the data. The latitudinal variation is represented by a weighted least-squares polynomial in the sine of the latitude. This method provides an improved numerical representation of the atmospheric noise with fewer coefficients than were required previously.

Key words: atmospheric noise, HF radio propagation, ionospheric predictions, least-squares fit, numerical maps, universal time.

1. INTRODUCTION

The transmission of useful information over a communication circuit by a radio signal is partially dependent upon the radio noise power encountered at the receiving station. The minimum required signal level at the receiver location, determined by the excess of the received signal power over the external noise power, differs for various grades and types of service. The three major types of external noise that the high-frequency (HF) radio signal must compete with are atmospheric, man-made, and galactic. Numerical representations of these noise sources are evaluated in the Institute for Telecommunication Sciences

HF Radio Prediction Computer Program (Barghausen et al, 1969)^{1/} to determine the expected noise power. The specific quantity evaluated, F_{am} at 1 MHz, is the median hourly value of F_a , where

$$F_a = 10 \log_{10} (p_n / kT_o b), \quad (1)$$

p_n = atmospheric noise power available from an equivalent loss-free antenna in a bandwidth b ,

k = Boltzmann's constant = 1.38×10^{-23} Joules per degree K,

T_o = reference temperature = 288° K,

b = effective receiver noise bandwidth in Hz.

Thus F_a represents the noise power density per cycle in decibels above kT_o (the noise power density in watts/cycle from a passive resistance at temperature T_o). The value p_n is the noise power available from a short vertical lossless receiving antenna. This antenna receives the radio noise from all azimuths, so that the noise power recorded is an integrated value of the noise received from all directions.

The numerical representation of F_{am} previously used in the computer predictions program was developed by Lucas and Harper (1965). Their representation consists of 24 numerical maps: one for each of six 4-hour time blocks (in local time, LT) and each of four 3-month periods. A numerical map (or numerical representation) is a finite series of mathematical terms, each consisting of a product of a numerical coefficient

^{1/} Hereafter this report is referred to as the Computer Predictions Program.

and an analytic function of the geographic coordinates. By using the numerical map, one can compute a value of F_{am} at any geographic location. The numerical maps of Lucas and Harper are based on a two-dimensional Fourier analysis (in latitude and longitude) of the basic radio noise data used to produce the world maps in CCIR Report 322 (CCIR, 1963). Lucas and Harper used 464 coefficients for each time block, thus requiring a total of 2,784 coefficients for a single 3-month period. The diurnal variation was obtained by linear interpolation between the numerical map values taken at the central hour of each time block. Seasonal variation was represented by a step function, thus producing discontinuities at certain times.

This report describes an improved numerical mapping of atmospheric radio noise. Based on an analysis of the same basic data (CCIR, 1963), the new worldwide numerical representations are in universal time (UT), thus reducing inconsistencies in the basic input data near the poles that result from the use of local time. Greater computing efficiency is attained with the UT maps since, for most applications, calculations are made for fixed instants of UT. By a careful analysis of residuals, we determined that an adequate representation can be obtained for each 3-month period with only 960 coefficients. This reduction (by two-thirds) from the number of coefficients used by Lucas and Harper (1965) provides significant saving in computer time and computer storage. The diurnal variation is represented by a smooth Fourier series (in place of linear interpolation) and the seasonal variation by linear interpolation (instead of a step function).

Sections 2 through 5 describe the mapping procedures. A discussion of the mapping residuals is given in section 6 and examples of world contour maps of atmospheric noise in UT are given in section 7.

2. CONVERSION OF DATA FROM LOCAL TIME TO UNIVERSAL TIME

The values of F_{am} , used as basic input data for a given time block and a 3-month period, are given at the 8,400 points (λ_m, θ_n) of a grid, where

$$\lambda_m = 90 - 1.8(m - \frac{1}{2}), \quad m = 1, 2, \dots, 100, \quad (2)$$

$$\theta_n = \frac{360}{84} (n - \frac{1}{2}), \quad n = 1, 2, \dots, 84. \quad (3)$$

Here λ denotes latitude, $-90^\circ \leq \lambda \leq 90^\circ$, and θ denotes longitude, $0^\circ \leq \theta \leq 360^\circ$. The input value of F_{am} at (λ_m, θ_n) is denoted by $y_{m,n}$. These data, the same as those used to prepare the LT maps in CCIR 322, were available for each of the six time blocks 0000-0400, 0400-0800, 0800-1200, 1200-1600, 1600-2000, and 2000-2400 in LT and for each of the 3-month seasonal periods December-February, March-May, June-August, and September-November. The data for each time-block were assumed to represent the central hour, so that the diurnal variation was defined at the 6 hours 0200, 0600, 1000, 1400, 1800, 2200, in LT. By Fourier analysis of data for these six hours, we obtained at each point (λ_m, θ_n) a continuous diurnal representation in the form

$$a_0 + \sum_{j=1}^2 \left[a_j \cos jt + b_j \sin jt \right] + a_3 \cos 3t, \quad (4)$$

where t denotes LT hour angle. An example of such a Fourier representation is shown in figure 1. The six data values (shown by x) are represented exactly by the Fourier representation. By means of the Fourier representation, we compute values $y_{m,n}^{(h)}$ of F_{am} for each of the UT hours $h = 0000, 0400, 0800, 1200, 1600, 2000$, at each of the 8,400 grid points (λ_m, θ_n) .

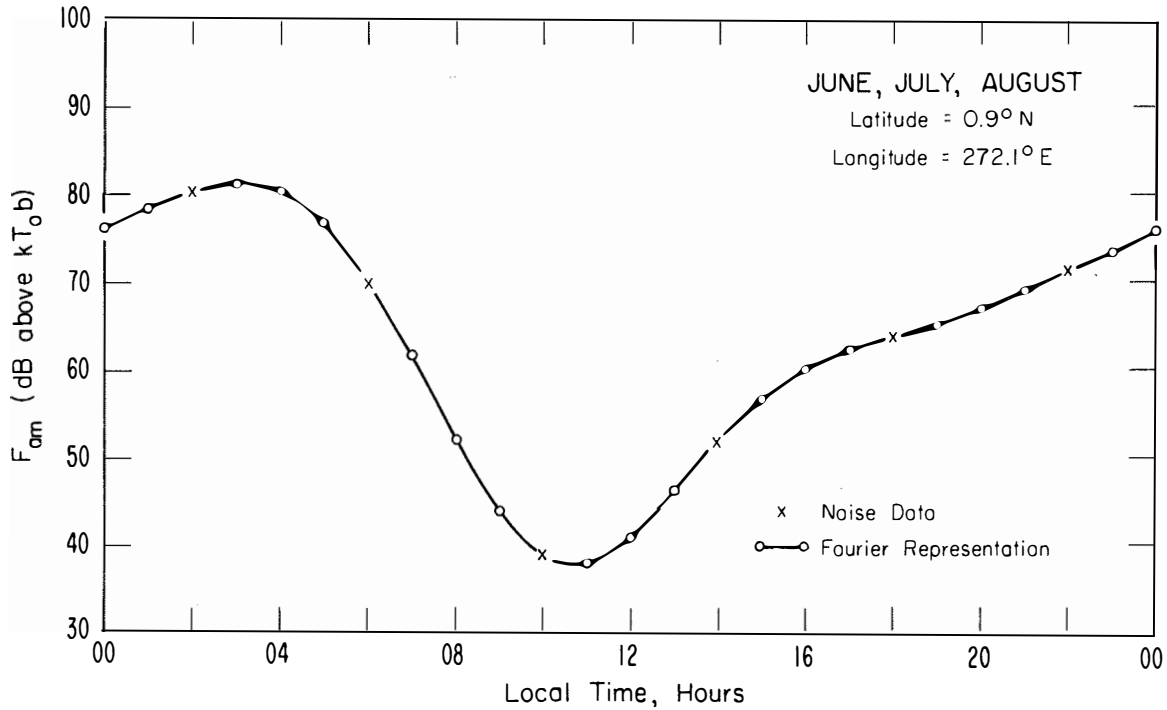


Figure 1. Fourier representation of diurnal variation of atmospheric noise data.

3. FOURIER ANALYSIS OF THE LONGITUDINAL VARIATION FOR A FIXED LATITUDE

Here and in the following section we deal with the problem of representing the worldwide geographic variation of the atmospheric noise parameter F_{0m} for a fixed hour of UT and a fixed 3-month season. The data $y_{m,n}^{(h)}$ are given at the 8,400 points (λ_m, θ_n) of the grid field for the fixed UT hour (h) by the method used in section 2. In this section we hold the latitude λ_m fixed and consider the representation of the periodic function of longitude θ defined at 84 equally spaced points θ_n . Fourier analysis of the data $y_{m,n}^{(h)}$ at these points yields an expression of the form

$$Z_{h, m}(\theta) = a_{m, 0}^{(h)} + \sum_{j=1}^J \left[a_{m, j}^{(h)} \cos j\theta + b_{m, j}^{(h)} \sin j\theta \right], \quad (5)$$

where J denotes the number of harmonics ($2J + 1 \leq N = 84$).

The coefficients are defined by the relations

$$\begin{aligned} a_{m, 0}^{(h)} &= \frac{1}{N} \sum_{n=1}^N y_{m, n}^{(h)}, \\ a_{m, j}^{(h)} &= \frac{2}{N} \sum_{n=1}^N y_{m, n}^{(h)} \cos j\theta_n, \\ b_{m, j}^{(h)} &= \frac{2}{N} \sum_{n=1}^N y_{m, n}^{(h)} \sin j\theta_n. \end{aligned} \quad (6)$$

At the outset, it was not known precisely how many harmonics were needed to provide an adequate fit for the longitudinal variation. An analysis of the mapping residual and of the coefficients themselves was performed to aid in determining the number of harmonics to be used. For each fixed value of J , such that $2J + 1 \leq N = 84$, the function $Z_{h, m}(\theta)$ is a best approximation in the sense of least squares. That is, the sum of squares of residuals

$$D_{m, J}^2 = \sum_{n=1}^{84} \left[y_{m, n}^{(h)} - Z_{h, m}(\theta_n) \right]^2 \quad (7)$$

is a minimum with respect to all real-valued coefficients $a_{m, j}^{(h)}$ ($j = 0, 1, \dots, J$), $b_{m, j}^{(h)}$ ($j = 1, 2, \dots, J$).

The quantity

$$e_{m, J} = \left[\frac{D_{m, J}^2}{84 - 2J - 1} \right]^{\frac{1}{2}} \quad (8)$$

is used as an estimate of the standard deviation of the residuals, $84 - 2J - 1$ being the number of degrees of freedom remaining after subtracting one for each term in (5).

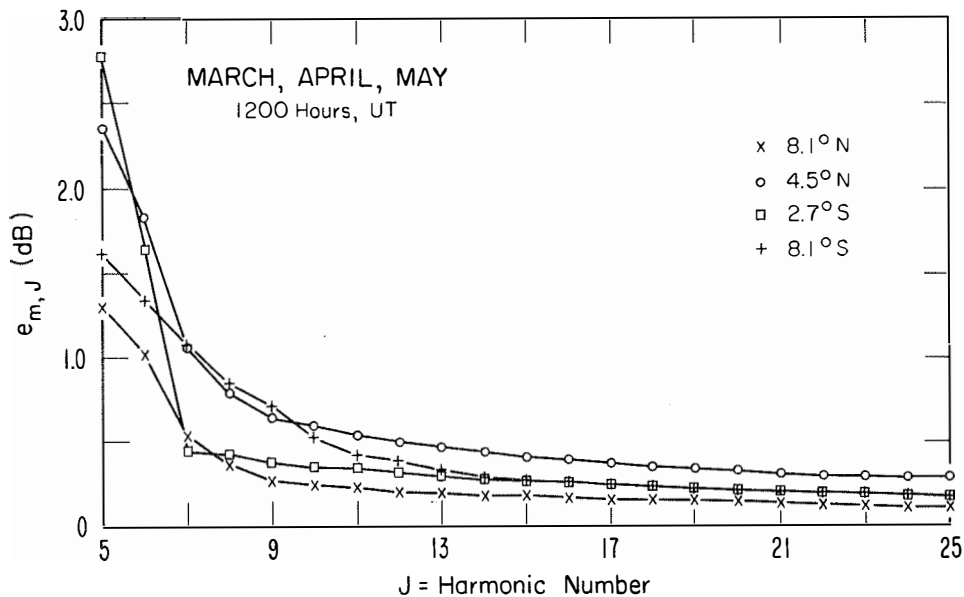


Figure 2. Standard deviation of residuals of longitudinal variation of atmospheric noise.

March, April, and May data for $h = 1200$ hours UT and four latitudes are plotted in figure 2 and illustrate how $e_{m,J}$ decreases with increasing values of J . The same type of analysis was performed for 22 other latitudes in the other three seasons. The latitudes chosen were those that produced the maximum residual when 144 latitudes from each of the four seasons were analyzed using harmonics only up to $J = 15$ or 18 . In figure 2 the quantity $e_{m,J}$ decreases rapidly from $J = 5$ to about $J = 9$ harmonics; $e_{m,J}$ continues to decrease as J increases beyond $J = 10$ but decreases at a slower rate.

In another type of analysis, to aid in determining the optimum number of harmonics, Fourier spectra are calculated using

$$\left[C_{m,j}^{(h)} \right]^2 = \left[a_{m,j}^{(h)} \right]^2 + \left[b_{m,j}^{(h)} \right]^2 \quad (9)$$

Average Fourier spectra (means of 100 values of $\left[C_{m,j}^{(h)} \right]^2$) are plotted against J on a log-log scale (e. g. figs. 3 and 4). Figure 3 is for the time block 1200-1600 LT, and figure 4 is for the time block 0800-1200 LT. Both are for the season June, July, and August. The number of harmonics to be used is usually indicated by the abscissa value where the slope of the Fourier spectrum approaches zero or oscillates about a line of zero slope (Jones and Gallet, 1962). In figure 3, the cutoff is at about $J = 17$.

The smooth decrease after $J = 7$ in the Fourier spectrum in figure 4 indicates that the basic atmospheric noise input data already have been smoothed. Plots of the Fourier spectra for individual latitudes indicate that this condition generally occurs in the Southern Hemisphere where very little observed data are available. The results in figures 2, 3, and 4, and additional similar analyses, have indicated that the Fourier series should be terminated after about the 10th harmonic. Thus $J = 10$ was chosen as the number of harmonics used to define $Z_{h,m}(\theta)$.

4. ANALYSIS OF LATITUDINAL VARIATION OF FOURIER COEFFICIENTS

The latitudinal variation of the Fourier coefficients $a_{m,j}^{(h)}$ and $b_{m,j}^{(h)}$ in (5) is represented by series of the form

$$\begin{aligned}
 a_{h,j}^{(\lambda)} &= \sum_{k=0}^K p_{j,k}^{(h)} G_{j,k}^{(\lambda)}, \quad j = 0, 1, \dots, J = 10 \\
 b_{h,j}^{(\lambda)} &= \sum_{k=0}^K q_{j,k}^{(h)} G_{j,k}^{(\lambda)}, \quad j = 1, 2, \dots, J = 10,
 \end{aligned}
 \tag{10}$$

where the functions $G_{j,k}^{(\lambda)}$ are defined by

$$G_{j,k}^{(\lambda)} = \sin^k \lambda \cos^j \lambda.
 \tag{11}$$

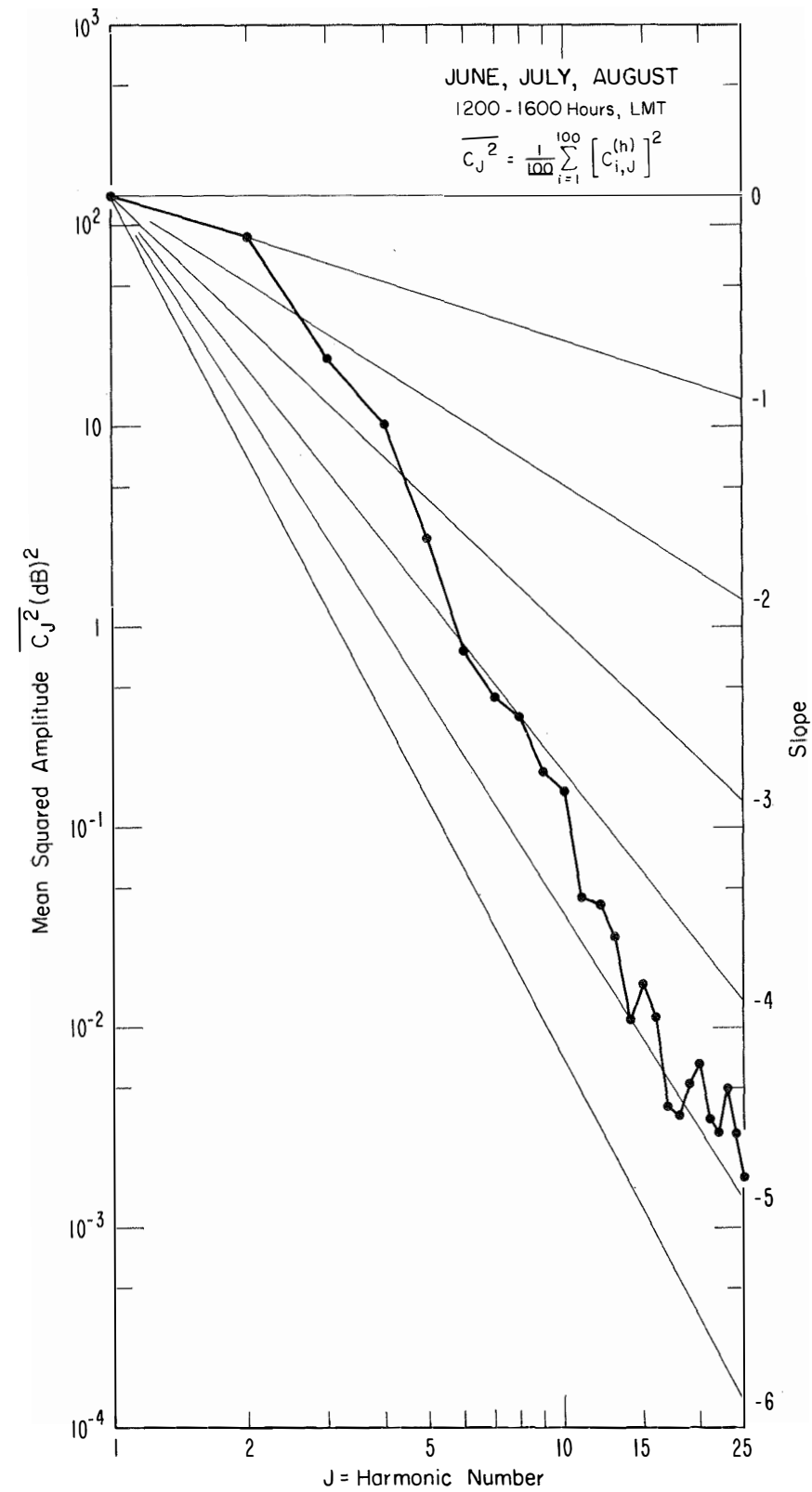


Figure 3. Average Fourier spectrum for longitudinal variation of atmospheric noise.

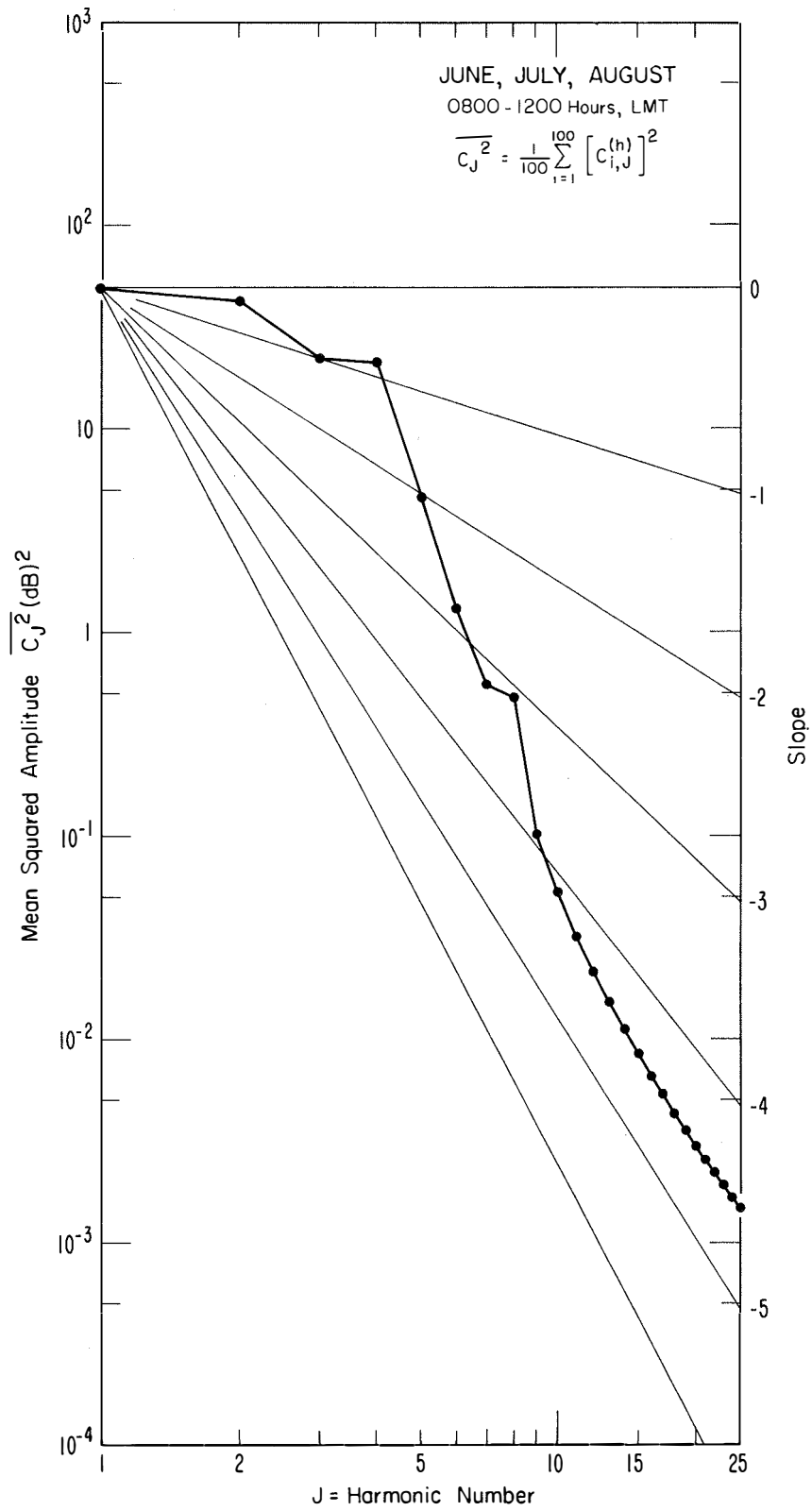


Figure 4. Average Fourier spectrum for longitudinal variation of atmospheric noise.

Here λ denotes the geographic latitude $-90^\circ \leq \lambda \leq 90^\circ$. The function $G_{j,k}(\lambda)$, $j \neq 0$ has a built-in constraint at the geographic poles ($\lambda = \pm 90^\circ$) in that the cosine factor is equal to zero. This property, similar to that of surface spherical harmonics, insures a well-defined single value of the functions defined by (10) at the poles. The coefficients $p_{j,k}^{(h)}$ and $q_{j,k}^{(h)}$ are determined by the method of least squares using the FORTRAN program NEQSOL (Jones et al., 1967).

The estimates of standard deviation of residuals

$$E_{j,K} = \left\{ \sum_{m=1}^{100} \left[a_{m,j}^{(h)} - a_{h,j}(\lambda_m) \right]^2 / (100-K-1) \right\}^{\frac{1}{2}}$$

$$F_{j,K} = \left\{ \sum_{m=1}^{100} \left[b_{m,j}^{(h)} - b_{h,j}(\lambda_m) \right]^2 / (100-K-1) \right\}^{\frac{1}{2}} \quad (12)$$

were used to measure the goodness of the approximation. Here $100-K-1$ is the number of degrees of freedom remaining after subtraction of one degree for each term in the series for $a_{h,j}(\lambda)$ or $b_{h,j}(\lambda)$. Values of $E_{j,k}$ and $F_{j,k}$ plotted against K are shown in figure 5 for 0800 UT, June-July-August, $j = 0, 1, 2, 3$, $K = 0, 1, 2, \dots, 19$. This analysis, similar to that illustrated by figure 2, indicates that a natural place for truncating the series occurs somewhere between $K=9$ and $K=14$. From a large number of similar analyses made for other hours and other seasons, we determined that $K=9$ is a good average cutoff, which is used for harmonics $0 \leq j \leq 7$. For harmonics $j = 8, 9$, and 10 , we chose the cutoff $K = 6$. Some examples of graphs of $E_{j,k}$ and $F_{j,k}$ for these harmonics are shown in figure 6 for the same season and hour of UT. These analyses show that an average cutoff of $K = 6$ for all harmonics would result in only a small increase in the variance of the residuals and would provide large

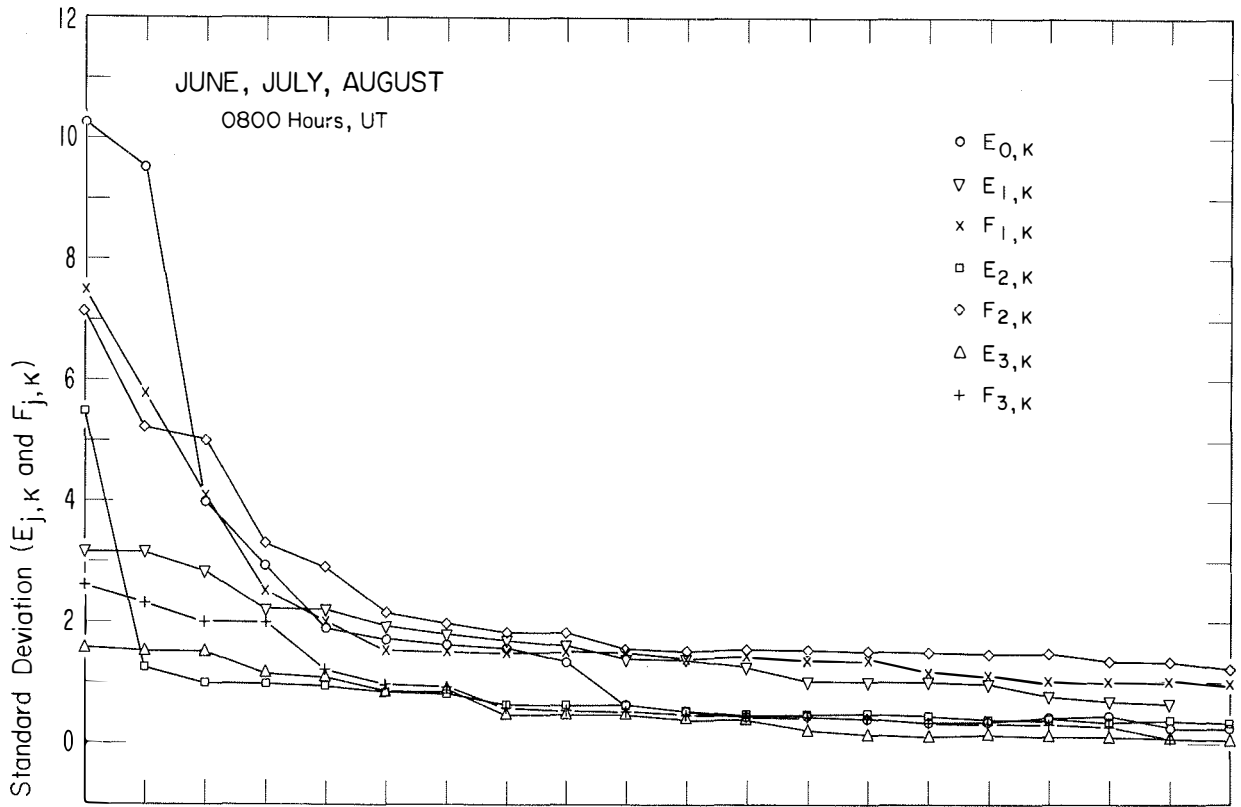


Figure 5. Standard deviation of residuals from latitudinal variation.

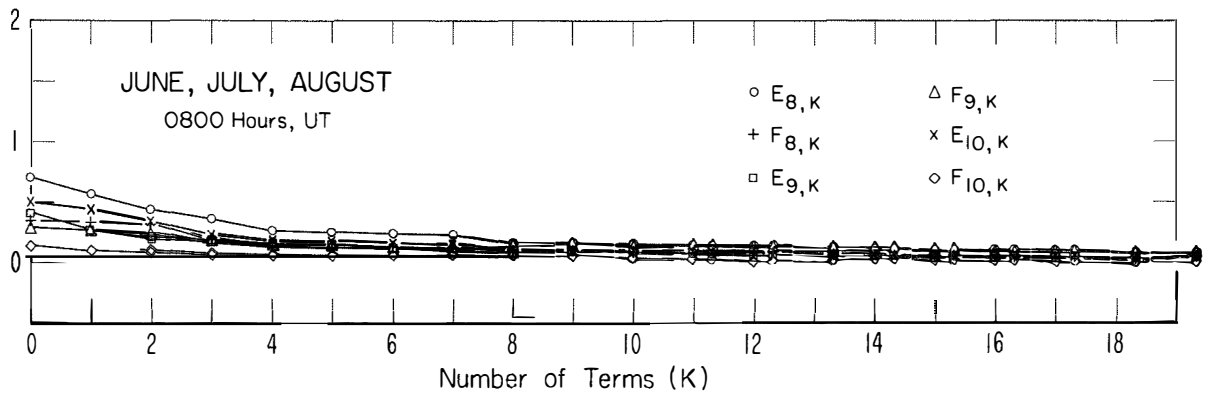


Figure 6. Standard deviation of residuals from latitudinal variation.

reductions in storage of coefficients and in computer time required to evaluate the numerical map. However, it would also result in maps that represent less detail in latitude variation, and hence was felt unjustified from the standpoint of the user's needs.

5. FOURIER ANALYSIS OF DIURNAL VARIATION WITHIN A THREE-MONTH PERIOD

Thus far we have described a representation of the two-dimensional geographic representation of F_{am} for a fixed UT = h and season. This representation has the form

$$X_h(\lambda, \theta) = \sum_{k=0}^K p_{0,k}^{(h)} G_{0,k}(\lambda) + \sum_{j=1}^{10} \left[\left(\sum_{k=0}^K p_{j,k}^{(h)} G_{j,k}(\lambda) \right) \cos j \theta + \left(\sum_{k=0}^K q_{j,k}^{(h)} G_{j,k}(\lambda) \right) \sin j \theta \right], \quad (13)$$

where $K = 9$ for $0 \leq j \leq 7$ and $K = 6$ for $j = 8, 9, 10$. For each 3-month season the diurnal variation of these representations is defined for the 6 hours of UT, $h = 0000, 0400, 0800, 1200, 1600, 2000$. The diurnal variation is represented by Fourier analysis of each of the coefficients $p_{j,k}^{(h)}$ and $q_{j,k}^{(h)}$. Thus we obtain expressions of the form

$$\begin{aligned}
P_{j,k}(T) &= \alpha_{j,k,0} + \sum_{i=1}^2 \left[\alpha_{j,k,i} \cos i T + \beta_{j,k,i} \sin i T \right] \\
&\quad + \alpha_{j,k,3} \cos 3 T, \\
Q_{j,k}(T) &= \gamma_{j,k,0} + \sum_{i=1}^2 \left[\gamma_{j,k,i} \cos i T + \delta_{j,k,i} \sin i T \right] \\
&\quad + \delta_{j,k,3} \cos 3 T.
\end{aligned} \tag{14}$$

Here T denotes the UT hour angle; $T = -180^\circ$ at the UT hour $h = 0000$ and $T = 0^\circ$ at 1200; T and h are related by

$$T = 15 h - 180^\circ, \quad -180^\circ \leq T \leq 180^\circ, \quad 00 \leq h \leq 24.$$

The Fourier coefficients are given by

$$\begin{aligned}
\alpha_{j,k,0} &= 1/6 \sum_h p_{j,k}^{(h)}, \\
\left. \begin{aligned}
\alpha_{j,k,i} &= 1/3 \sum_h p_{j,k}^{(h)} \cos i T_h, \\
\beta_{j,k,i} &= 1/3 \sum_h p_{j,k}^{(h)} \sin i T_h
\end{aligned} \right\} i = 1, 2 \\
\alpha_{j,k,3} &= 1/6 \sum_h (-1)^{h-1} p_{j,k}^{(h)},
\end{aligned} \tag{15}$$

$$\begin{aligned}
\gamma_{j,k,0} &= 1/6 \sum_h q_{j,k}^{(h)}, \\
\gamma_{j,k,i} &= 1/3 \sum_h q_{j,k}^{(h)} \cos i T_h, \\
\delta_{j,k,i} &= 1/3 \sum_h q_{j,k}^{(h)} \sin i T_h, \\
\gamma_{j,k,3} &= 1/6 \sum_h (-1)^{h-1} q_{j,k}^{(h)}.
\end{aligned}
\left. \vphantom{\begin{aligned} \gamma_{j,k,0} \\ \gamma_{j,k,i} \\ \delta_{j,k,i} \\ \gamma_{j,k,3} \end{aligned}} \right\} i = 1, 2 \quad (16)$$

Here \sum_h denotes a sum over $h = 0000, 0400, 0800, 1200, 1600, 2000$, and $T_h = 15h - 180^\circ$. The final form of a numerical map of F_{am} for a fixed 3-month season is given by

$$\begin{aligned}
Y(\lambda, \theta, T) &= \sum_{k=0}^K P_{0,k}(T) G_{0,k}(\lambda) \\
&+ \sum_{j=1}^{10} \left[\left(\sum_{k=0}^K P_{j,k}(T) G_{j,k}(\lambda) \right) \cos j \theta + \left(\sum_{k=0}^K Q_{j,k}(T) G_{j,k}(\lambda) \right) \sin j \theta \right], \quad (17)
\end{aligned}$$

where $K = 9$ for $0 \leq j \leq 7$ and $K = 6$ for $j = 8, 9, 10$.

6. THE MAPPING RESIDUALS

For each of the 6 hours of UT and each season, residuals were computed between values $y_{m,n}^{(h)}$ of F_{am} (sec. 2) and corresponding values computed from the numerical map (17). Table 1 shows values of the rms of 1260 of these residuals for each UT hour for each of the four seasons. This sampling consists of residuals at a rectangular array defined by the intersections of 42 equally spaced longitudes and 30 equally spaced latitudes between $\lambda = 81^\circ N$ and $\lambda = 81^\circ S$, or about one-sixth of the original grid of points. Since residuals at the high latitudes $|\lambda| > 81^\circ$ were considerably

Table 1. Comparison of rms (R) of 1, 260 Residuals for Four Different Analyses.

Hour (UT)	rms Residuals (dB)			
	Map A	Map B	Map C	Map D
December, January, and February				
0000	0.80	0.81	1.35	1.66
0400	0.73	0.74	1.29	1.53
0800	0.85	0.86	1.37	1.71
1200	0.82	0.84	1.38	1.84
1600	0.67	0.68	1.29	1.54
2000	0.66	0.67	1.26	1.41
March, April, and May				
0000	0.74	0.75	1.21	1.35
0400	0.72	0.72	1.19	1.34
0800	0.74	0.75	1.20	1.57
1200	0.77	0.78	1.23	1.74
1600	0.79	0.79	1.24	1.42
2000	0.68	0.68	1.16	1.30
June, July, and August				
0000	0.78	0.85	1.68	2.07
0400	0.87	0.95	1.74	2.11
0800	0.98	1.05	1.80	2.08
1200	0.90	0.94	1.73	1.94
1600	0.89	0.90	1.71	1.93
2000	0.83	0.87	1.69	1.97
September, October, and November				
0000	0.81	0.85	1.12	1.43
0400	0.78	0.80	1.08	1.45
0800	0.82	0.85	1.12	1.57
1200	0.98	1.04	1.27	1.69
1600	0.89	0.91	1.16	1.49
2000	0.82	0.84	1.11	1.28
Longitude, J =	15	10	10	10
Latitude, K =	14*	14*	14*	9*
Time, H =	2+#	2+#	2	2
Total numerical coefficients	2022	1602	1335	960

* When $J \geq 8$, $K = 6$

Six coefficients are used in the series to represent the diurnal variation including the cosine term for the third harmonic.

larger, they were omitted from these computations. This is due to the large variance in the original input data in the polar regions, possibly the result of mapping in local time and scanty high latitude observed data. Our numerical maps in UT effectively average the data in the polar regions and define unique values at the poles; thus they provide a self-consistent representation.

For comparison, we used four (A, B, C, and D) slightly different numerical maps in UT to compute the rms residuals shown in table 1. The maps differed in the cutoffs of the series, as described in sections 3, 4, and 5. Map A used $J = 15$ harmonics for longitude variation, whereas maps B, C, and D used $J = 10$. Maps A and B used six terms ($2\frac{1}{2}$ harmonics) for diurnal variation, whereas maps C and D used only five terms (two harmonics). For latitude variation (sec. 4), map A, B, and C used $K = 14$, whereas D used $K = 9$ for $0 \leq j \leq 7$; all four maps used $K = 6$ for $8 \leq j \leq J$. The values of these cutoff parameters are summarized at the bottom of the table along with the total number of coefficients.

As can be seen, the rms residuals for map A are only, at most, 0.08 dB less than those for map B even though 420 more coefficients are used to obtain the results for map A. This difference in rms residual appears to be negligible. The additional term in the diurnal Fourier series for map B makes a reduction in rms residual (compared with map C) of between 0.23 and 0.83 dB, and (compared with map D) of between 0.44 and 1.22. To economize in numerical coefficients and to obtain some diurnal smoothing, we decided to adopt map D. Thus, only 960 numerical coefficients are used to represent the atmospheric noise for a 3-month period as compared with 2,784 coefficients used by Lucas and Harper (1965).

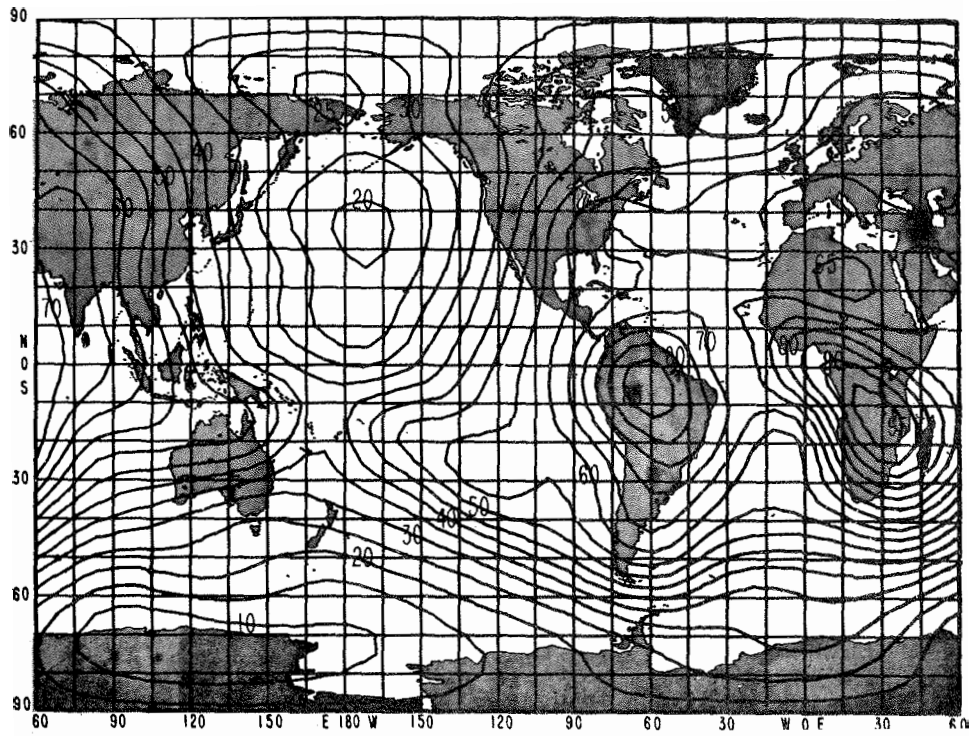
7. WORLD MAPS OF THE 1 MHz ATMOSPHERIC NOISE IN UNIVERSAL TIME

Using a computer evaluation of the numerical maps, one can produce UT contour maps of F_{am} in dB above kT_o directly on a cathode-ray tube plotter. The maps shown in figures 7 through 9 are for January, and the maps shown in figures 10 through 12 are for July. They are each plotted from a grid of 1,702 points consisting of 46 columns equally spaced in longitude and 37 rows equally spaced in latitude. The maps are for individual months rather than for a 3-month season, as in C. C. I. R. 322 where summer, for instance, includes June, July, and August in the Northern Hemisphere, and December, January, and February in the Southern Hemisphere. Since some HF networks are essentially worldwide, it is often useful to have the atmospheric noise represented simultaneously over the surface of the earth.

In the computer predictions program, numerical coefficients represent each month of the year. This was achieved by assuming the central month of each 3-month period (i. e., January, April, July, and October) to be the mean month for that period. A linear interpolation was then used to provide numerical coefficients for the remaining 8 months of the year. A Fourier series could have been used to represent the seasonal variation; however, we decided that the data did not warrant such a complete treatment, and the more simple linear interpolation was used instead.

The atmospheric noise maps are given here at 1 MHz, whereas in the computer predictions, the primary range of interest is about 1 to 30 MHz. The curves in C. C. I. R. Report 322 that give the variation of atmospheric noise with frequency and the curves that give noise variability, both as a function of LT and season, can still be used in the computer predictions. Moreover, note that UT contour maps of atmospheric noise now can be produced at any desired frequency.

0000 Hours, Universal Time



0400 hours, Universal Time

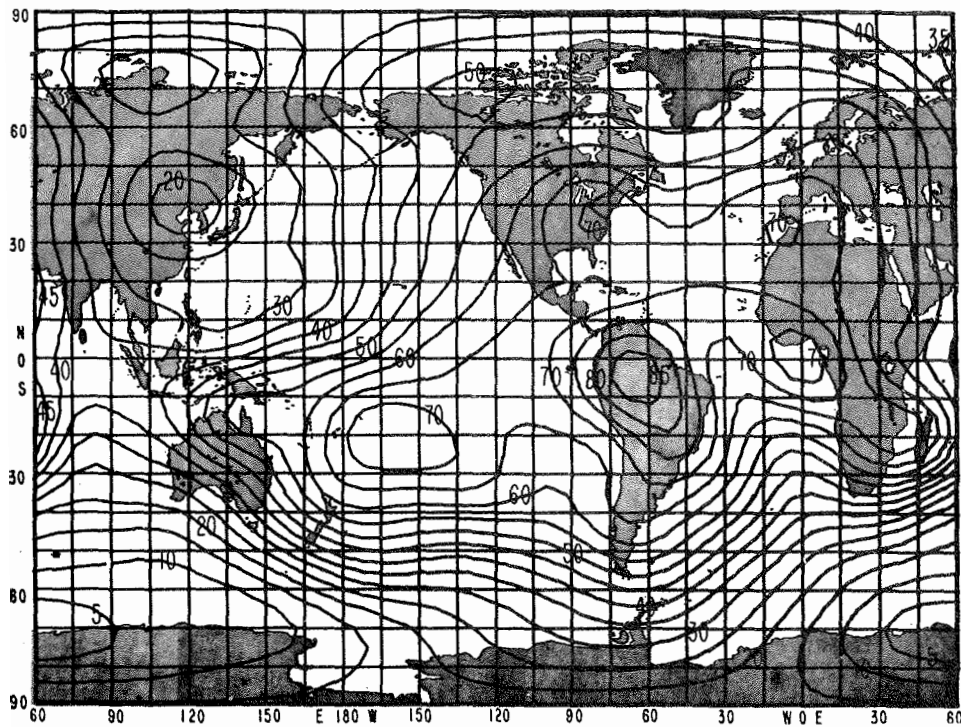
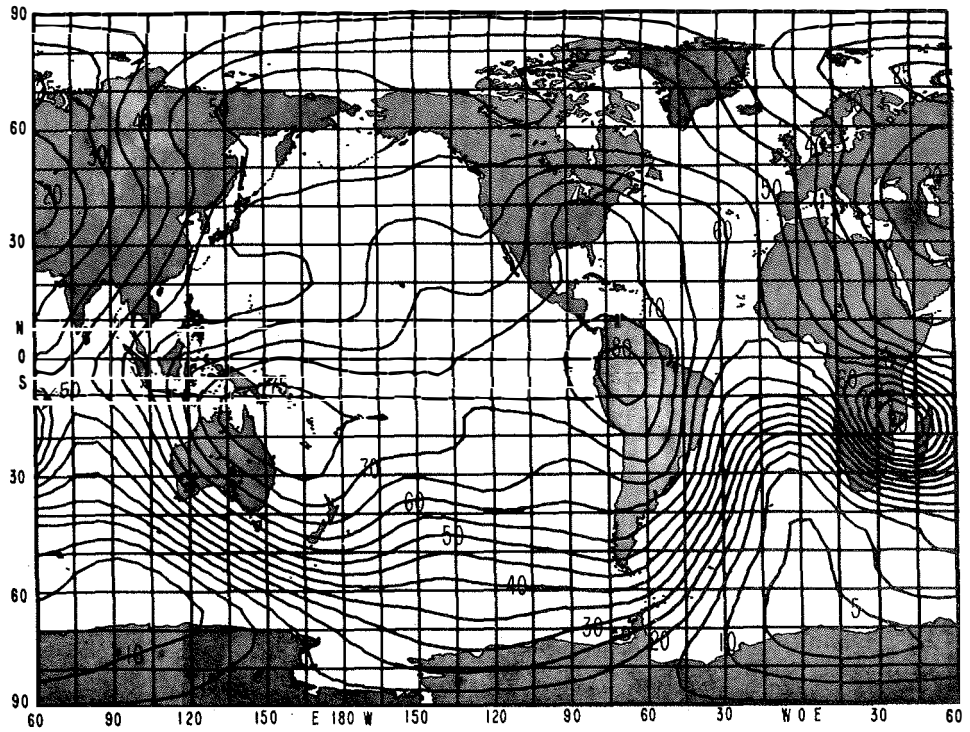


Figure 7. 1 MHz atmospheric noise (F_{am} in dB above kT_0 b) computed by numerical maps for January.

0800 Hours, Universal Time



1200 Hours, Universal Time

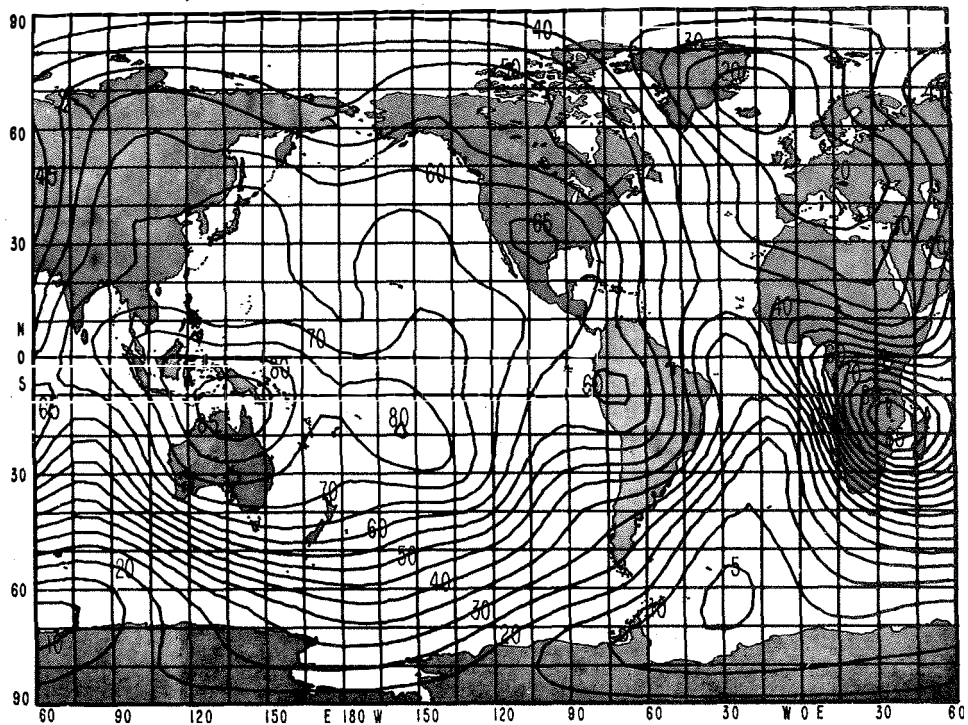
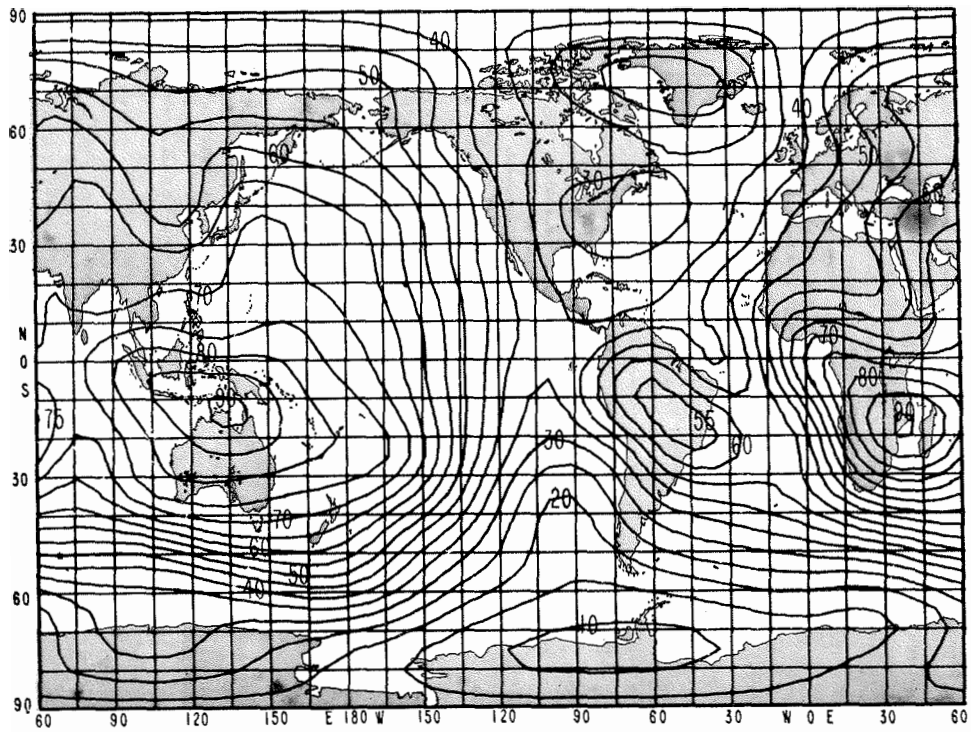


Figure 8. 1 MHz atmospheric noise (F_{am} in dB above kT_0b) computed by numerical maps for January

1600 Hours, Universal Time



2000 Hours, Universal Time

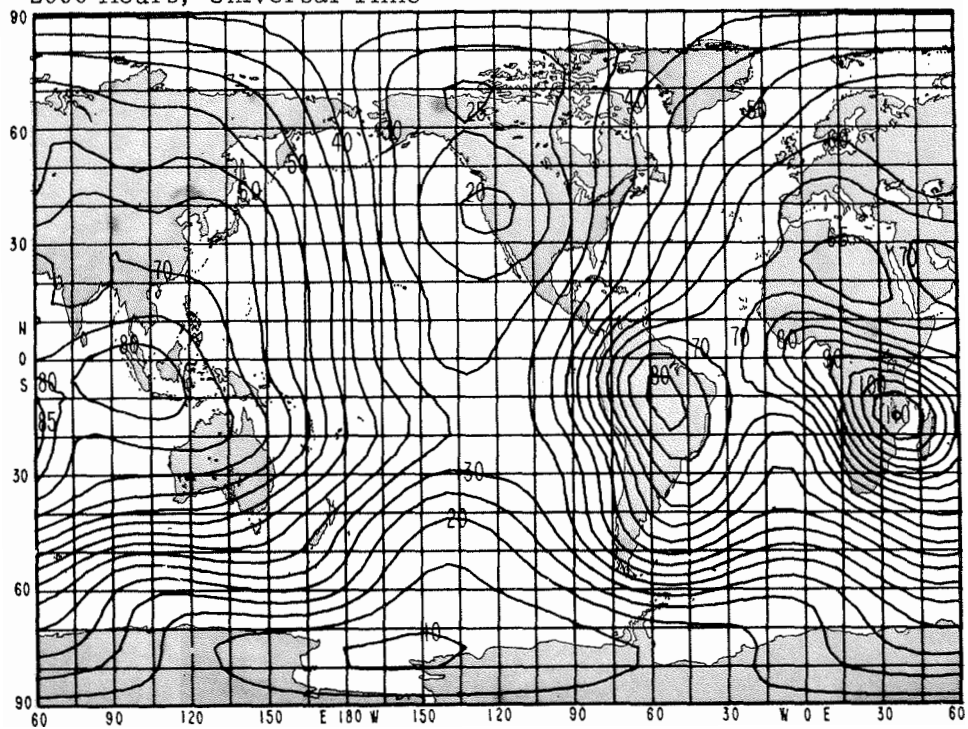
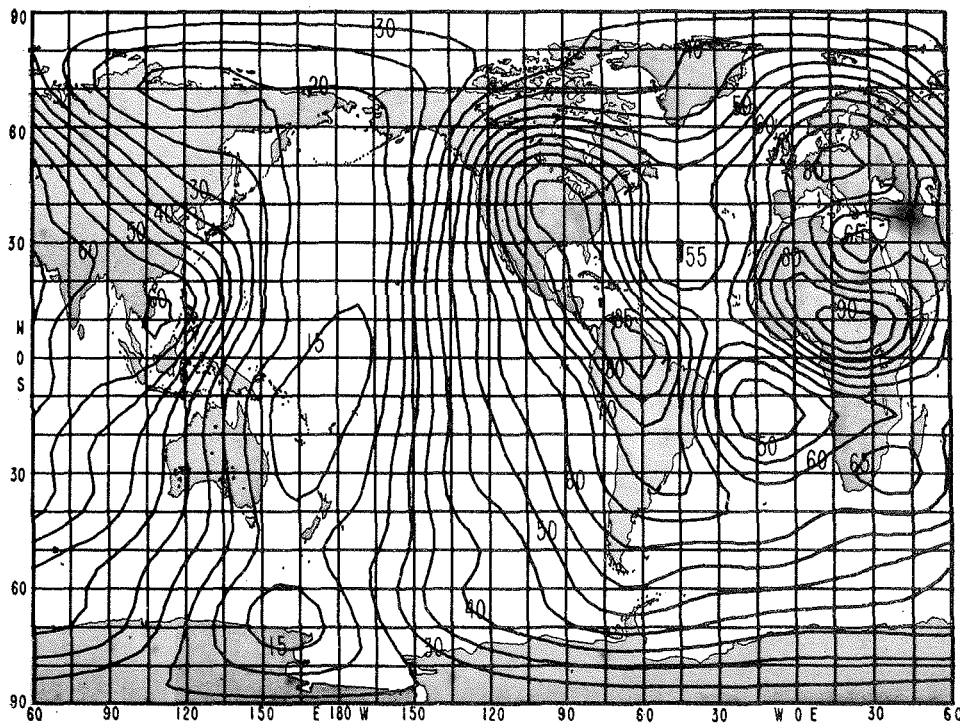


Figure 9. 1 MHz atmospheric noise (F_{am} in dB above $kT_0 b$) computed by numerical maps for January

0000 Hours, Universal Time



0400 Hours, Universal Time

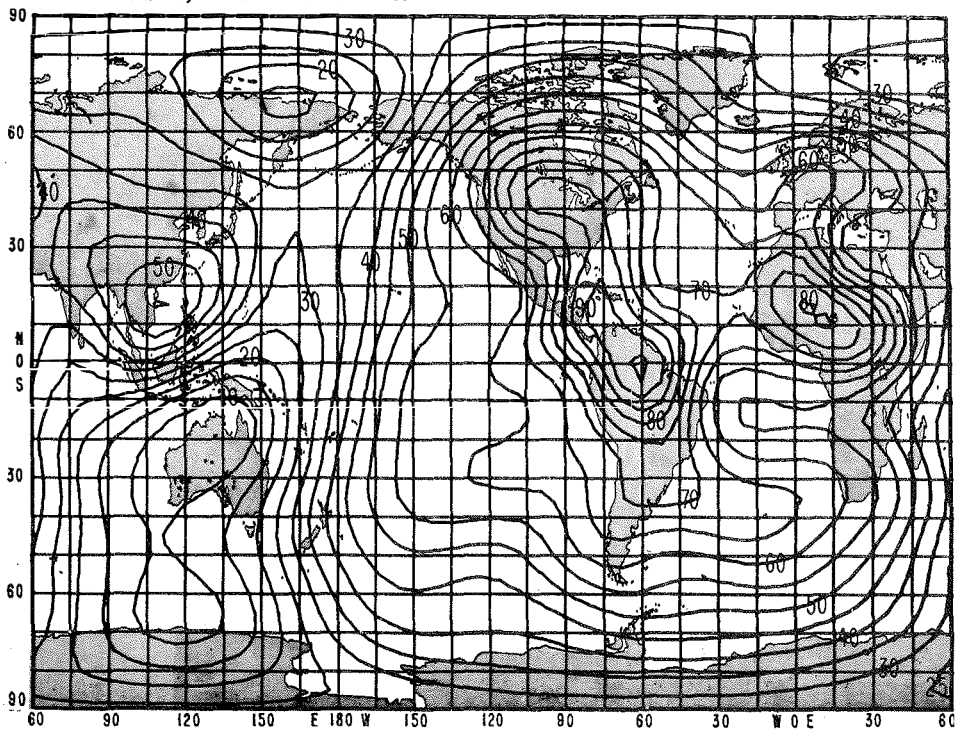
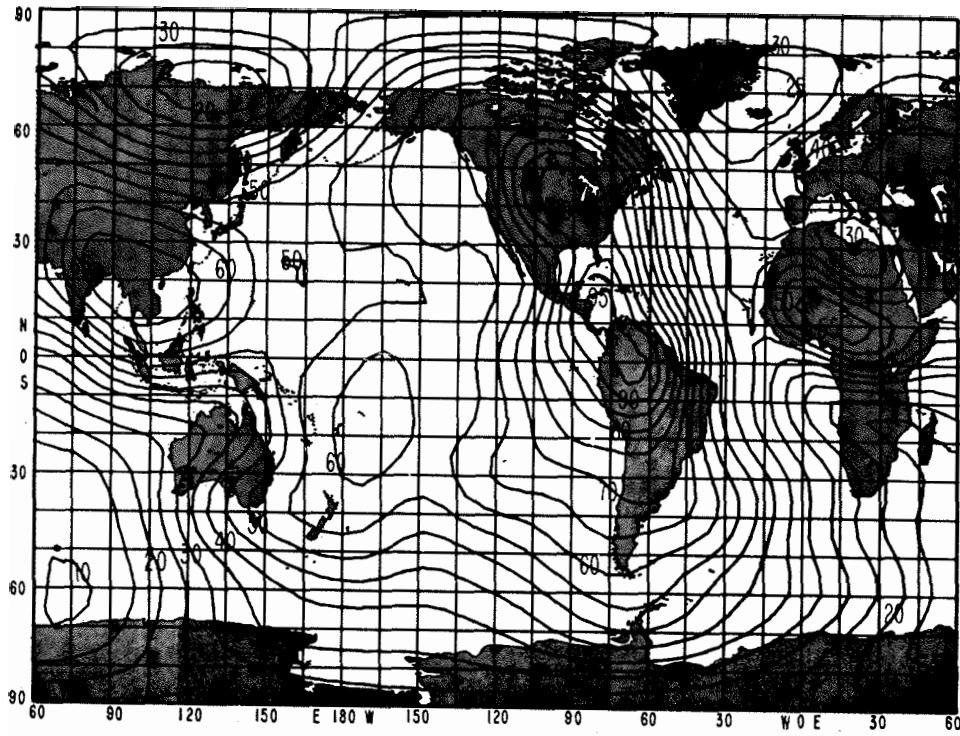


Figure 10. 1 MHz atmospheric noise (F_{am} in dB above kT_0) computed by numerical maps for July.

0800 Hours, Universal Time



1200 Hours, Universal Time

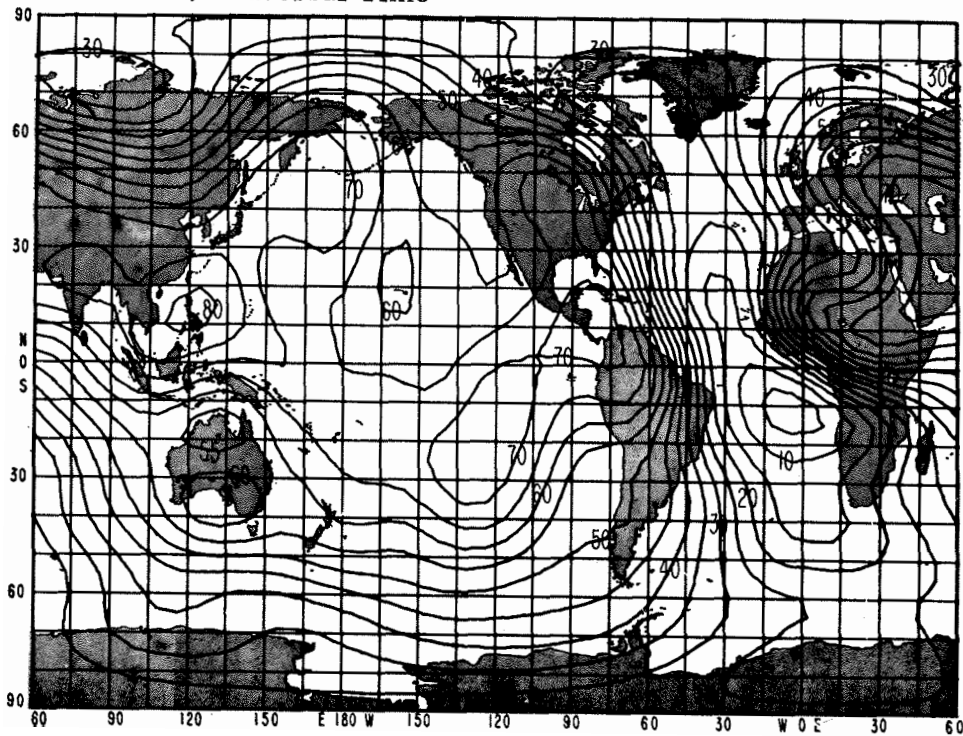
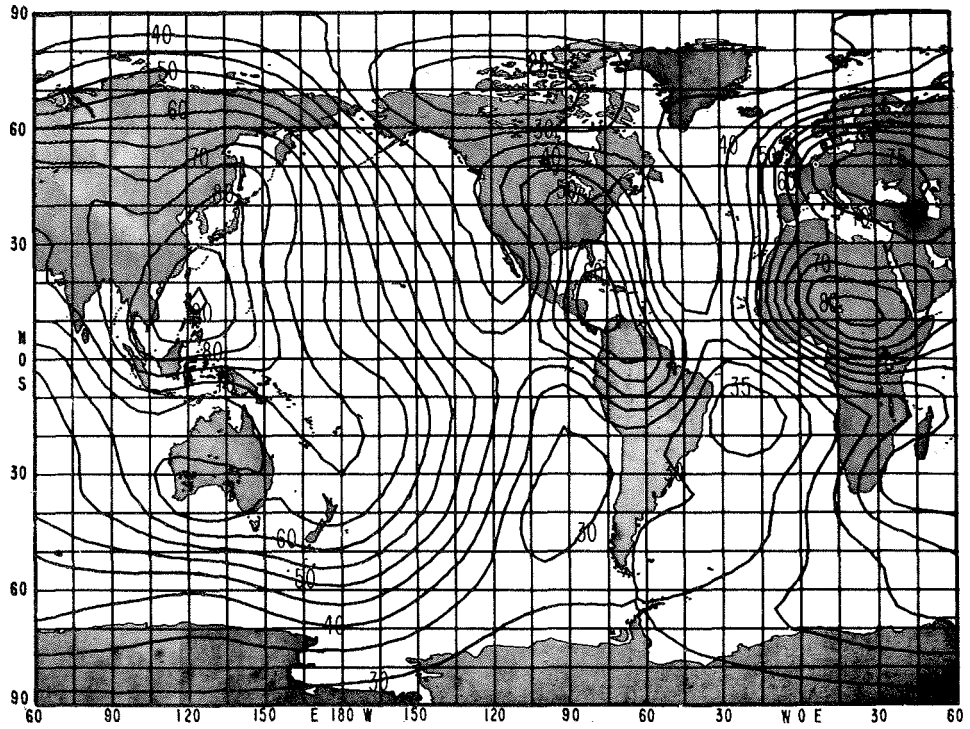


Figure 11. 1 MHz atmospheric noise (F_{am} in dB above kT_{0b}) computed by numerical maps for July.

1600 Hours, Universal Time



2000 Hours Universal Time

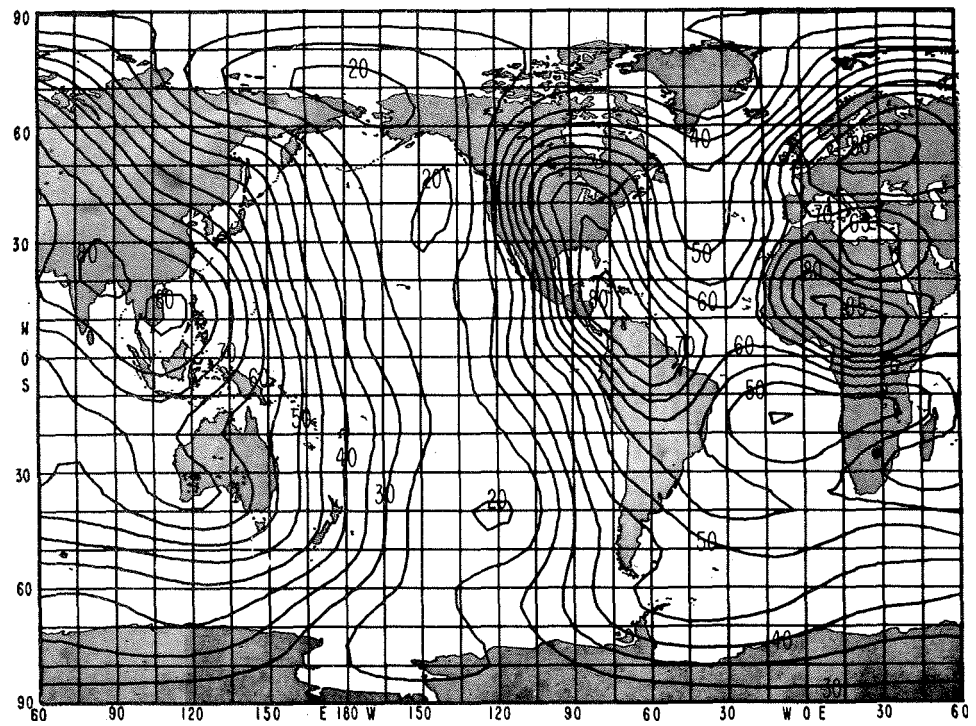


Figure 12. 1 MHz atmospheric noise (F_{am} in dB above kT_0) computed by numerical maps for July.

Table 2. Sample of the 1 MHz Atmospheric Noise Numerical Map Coefficients for January.

J	K	I = 1	I = 2	I = 3	I = 4	I = 5
1	1	6.1907248+1	2.1037982+0	8.2413481-1	-1.1031124+0	-1.5030747-1
1	2	-2.9271312+1	1.6142382-1	2.3081261-1	1.8632565+0	1.4331215+0
1	3	-3.2471149+1	-2.5715698-2	5.0232658+0	6.5333559+0	-2.0624520+0
1	4	1.7611225+2	-2.1000601+1	6.6000082+0	-2.7274801+1	-1.4414027-1
1	5	2.8033548+0	1.1002193+1	-3.8324998+1	-3.4533068+0	9.5397198+0
1	6	-3.8834455+2	5.0678955+1	-1.7801085+1	8.4614009+1	-1.0876950+0
1	7	-2.6570585+1	-2.5227614+1	6.0959533+1	-1.4191762+1	-1.4571493+1
1	8	4.5312036+2	-4.0817397+1	1.5280057+1	-9.5564974+1	-1.8240825+0
1	9	2.2074332+1	1.2680329+1	-2.8833439+1	1.2155956+1	7.3397780+0
1	10	-2.0049331+2	1.0583700+1	-4.5281172+0	3.6317077+1	1.6587898+0
2	1	1.9982258+0	1.9815713+1	5.2506663+0	-7.5949625-1	1.4179486+0
2	2	-1.5608785+1	4.7352736+0	-1.3368053+1	3.9502288+0	1.7047314+0
2	3	1.9591513+1	-2.8175296+1	-3.4783705+1	-1.5448676+0	-2.4777859+1
2	4	9.8625196+1	-2.0315051+1	5.1142886+1	-1.5037678+1	-1.7468240+1
2	5	-1.2149510+2	3.1679959+2	1.9725006+2	9.0614909+0	9.9714967+1
2	6	-2.7877336+2	6.9161467+1	-2.2805563+2	-9.2680359+0	9.0502046+1
2	7	1.8053694+2	-6.8786918+2	-3.7429384+2	-5.1954989+0	-1.4185593+2
2	8	4.2653765+2	-1.4213744+2	4.0925314+2	7.2017240+1	-1.5584497+2
2	9	-8.2590342+1	4.4298704+2	2.2524171+2	-3.6922586+0	6.6500374+1
2	10	-2.3138389+2	9.7610014+1	-2.2665185+2	-5.4789354+1	8.5123688+1
3	1	4.3126886+0	4.2044896+0	-2.0482632+1	-1.6174159+0	6.0394529-1
3	2	1.9076338+0	-1.9492324+1	-6.8841750+0	1.1918393+1	1.7864891+0
3	3	-3.5350152+1	-2.2192816+1	3.7312204+1	9.4199146+0	-9.2556133+0
3	4	3.5884841+1	8.1677054+1	3.4440142+1	-9.2046690+1	-2.6531548+1
3	5	8.2536010+1	1.7357469+2	-3.3277123+2	-1.0697376+1	5.0127298+1
3	6	-7.4591441+1	-3.1645037+2	-9.9952683+1	2.9094797+2	6.6405240+1
3	7	-9.8995967+1	-3.6175003+2	6.5735339+2	-1.0257727+1	-9.7347833+1
3	8	5.3721503+1	5.2983726+2	1.4212980+2	-3.7665773+2	-7.1122753+1
3	9	4.5969423+1	2.2578270+2	-4.0069058+2	1.3035434+1	5.9473946+1
3	10	-1.5654180+1	-2.8375280+2	-7.6713989+1	1.6955392+2	3.1080310+1
4	1	-2.1639590+0	-9.0986609-1	1.2014325+0	3.7662582+0	3.8942825+0
4	2	-3.5907916+0	-2.4207567+0	-3.6824810+0	1.6565712+1	-3.6628332+0
4	3	3.1113054+1	-2.5913751+1	-1.2553440+0	-1.7467697+1	-1.3864255+1
4	4	-4.8982771+1	5.1112413+1	1.0019917+0	-1.3351220+2	-2.5640973+1
4	5	-1.2840516+2	1.7791442+2	-5.3793211+1	1.9047903+2	1.3113409+2
4	6	3.0586619+2	-1.8796142+2	8.8750311+1	5.7008299+2	1.2087435+2
4	7	1.1658111+2	-3.8473635+2	1.4413479+2	-4.0315089+2	-3.0943131+2
4	8	-5.2447242+2	2.3566793+2	-2.7123466+2	-9.9167684+2	-2.3840747+2
4	9	4.8588078+0	2.5931291+2	-9.3250516+1	2.5504893+2	2.1751716+2
4	10	2.9022210+2	-8.7843471+1	1.9215480+2	6.2517043+2	1.7932927+2
5	1	-3.7303515-1	7.2450852-1	8.4600023-1	2.7464576+0	-4.1496186+0
5	2	-6.0114478+0	9.5846386+0	-1.2284086+0	4.3195171-1	-9.7088661+0
5	3	8.4044072+0	-1.0389190+0	-4.5306762+0	9.6038017-1	-1.1333358+1
5	4	-9.8537934+0	-1.1145838+2	2.6912214+1	-6.7823304+1	9.0195058+1
5	5	-4.2706750+1	2.5879060+1	-4.7766255+0	8.7679488+1	-5.6778551+0
5	6	1.3985714+2	4.4810736+2	-1.1757032+2	2.5888991+2	-5.2760883+2
5	7	7.4340768+1	-5.9618349+1	7.7679302+1	-2.5860768+2	5.5015037+1
5	8	-2.9126505+2	-7.1500039+2	1.2266829+2	-4.2444157+2	1.0516350+3
5	9	-4.3270769+1	3.5424150+1	-8.8452175+1	1.9258684+2	-5.0717023+1
5	10	1.7170760+2	3.7158176+2	-3.8030089+1	2.6313984+2	-6.9623406+2

The 1 MHz atmospheric noise numerical map coefficients for the 12 months, January through December, are incorporated in the Computer Predictions Program. A sample page of the coefficients for part of January is shown in table 2 in a FORTRAN "E12,7" format. For a more compact printout, zeros preceding the exponents of the coefficients have been removed. The coefficients in the columns labeled "J", "K", and "I" (see for example table 2) correspond for each month to $\alpha_{j,k,i}$, $\beta_{j,k,i}$, $\gamma_{j,k,i}$ and $\delta_{j,k,i}$ in (14) as shown in table 3.

Table 3. Diagram of the Atmospheric Noise Numerical Map Coefficients.

<u>J</u>	<u>K</u>	<u>I = 1</u>	<u>I = 2</u>	<u>I = 3</u>	<u>I = 4</u>	<u>I = 5</u>
1	1	$\alpha_{0,0,0}$	$\alpha_{0,0,1}$	$\beta_{0,0,1}$	$\alpha_{0,0,2}$	$\beta_{0,0,2}$
⋮	⋮	⋮	⋮	⋮	⋮	⋮
1	10	$\alpha_{0,9,0}$	$\alpha_{0,9,1}$	$\beta_{0,9,1}$	$\alpha_{0,9,2}$	$\beta_{0,9,2}$
2	1	$\alpha_{1,0,0}$	$\alpha_{1,0,1}$	$\beta_{1,0,1}$	$\alpha_{1,0,2}$	$\beta_{1,0,2}$
⋮	⋮	⋮	⋮	⋮	⋮	⋮
2	10	$\alpha_{1,9,0}$	$\alpha_{1,9,1}$	$\beta_{1,9,1}$	$\alpha_{1,9,2}$	$\beta_{1,9,2}$
3	1	$\gamma_{1,0,0}$	$\gamma_{1,0,1}$	$\delta_{1,0,1}$	$\gamma_{1,0,2}$	$\delta_{1,0,2}$
⋮	⋮	⋮	⋮	⋮	⋮	⋮
3	10	$\gamma_{1,9,0}$	$\gamma_{1,9,1}$	$\delta_{1,9,1}$	$\gamma_{1,9,2}$	$\delta_{1,9,2}$
⋮	⋮	⋮	⋮	⋮	⋮	⋮
20	1	$\alpha_{10,0,0}$	$\alpha_{10,0,1}$	$\beta_{10,0,1}$	$\alpha_{10,0,2}$	$\beta_{10,0,2}$
⋮	⋮	⋮	⋮	⋮	⋮	⋮
20	10	$\alpha_{10,6,0}$	$\alpha_{10,6,1}$	$\beta_{10,6,1}$	$\alpha_{10,6,2}$	$\beta_{10,6,2}$
21	1	$\gamma_{10,0,0}$	$\gamma_{10,0,1}$	$\delta_{10,0,1}$	$\gamma_{10,0,2}$	$\delta_{10,0,2}$
⋮	⋮	⋮	⋮	⋮	⋮	⋮
21	10	$\gamma_{10,6,0}$	$\gamma_{10,6,1}$	$\delta_{10,6,1}$	$\gamma_{10,6,2}$	$\delta_{10,6,2}$

The reader should be cautioned that the indexes "J" and "K" used in table 3 have a different meaning from that used in sections 3 and 4. These coefficients for one month are contained in five pages similar to those shown in table 2. January through December require sixty pages.

The FORTRAN computer subroutine EVALUTAN, used to evaluate the numerical maps, is listed in Appendix A. The array containing the coefficients in COMMON /A/ is identified as ABGD(21, 10, 5), and is indexed as ABGD(J, K, I) in the program. The indexes "I", "J", and "K" correspond directly to the column headings used in tables 2 and 3.

A card deck, listing, or magnetic tape, containing the numerical coefficients for all twelve months of the year can be supplied at cost on request from the following address:

Office of Telecommunications
Institute for Telecommunication Sciences
Boulder Laboratories
Boulder, Colorado 80302

8. CONCLUSIONS

The numerical maps described in this report provide a number of improvements in the representation of atmospheric noise. The number of numerical coefficients required to represent each 3-month period has been reduced by 1,824 (65.5 percent) compared with those for numerical maps previously used. Therefore, fewer storage locations are required in the Computer Predictions Program, and less time is required for the computer calculations.

The contour maps can now be produced in UT, which gives a synoptic picture of the atmospheric noise over the surface of the earth. The functions used in mapping the parameter F_{am} also provide a continuous UT representation at the poles. This is a more realistic way of

looking at atmospheric noise, since many high-frequency radio networks are essentially worldwide systems. We also now have the computer capability of producing the UT world contour maps of atmospheric noise at any frequency in the HF range for any hour of the day or for any month of the year.

The original numerical representation of the noise was continuous only in latitude and longitude. The new representation is continuous in time as well, and some smoothing is incorporated in the diurnal variation.

Previously the coefficients for a 3-month season were used for each month in the period. This resulted in a step function between periods. A linear interpolation has now been incorporated, resulting in a unique set of coefficients for each month, thus removing the step function from the seasonal variation.

The Fourier series in longitude and time are orthogonal so that the coefficients in the computed series are unchanged if higher order harmonics are added or lower order harmonics are deleted. The reader must be cautioned, however, that the functions used in (12), the latitude analysis, are not orthogonal. If terms are cut off the end of the series, the whole series must be recomputed.

9. REFERENCES

- Barghausen, A. F., J. W. Finney, L. L. Proctor, and L. D. Schultz (1969), Predicting long-term operational parameters of high-frequency sky-wave telecommunication systems, ESSA Tech. Rept. ERL 110-ITS 78 (U. S. Government Printing Office, Washington, D. C. 20402).
- C. C. I. R. (1963), World distribution and characteristics of atmospheric radio noise, Report 322, Documents of the Xth Plenary Assembly, Geneva 1963.
- Jones, W. B. and R. M. Gallet (1962), The representation of diurnal and geographic variations of ionospheric data by numerical methods, ITU Telecomm. J. 29, No. 5, 129-149; also published (July-August 1962) Journal of Research NBS 66D (Radio Propagation, No. 4, 419-438).
- Jones, W. B., D. L. Obitts, R. M. Gallet, and G. deVaucouleurs (1967), Application of numerical methods of mapping to astronomical surface photometry, ESSA Tech. Rept. IER 25-ITSA 25 (U. S. Government Printing Office, Washington, D. C. 20402).
- Lucas, D. L. and J. D. Harper, Jr. (1965), A numerical representation of C. C. I. R. Report 322 high frequency (3-30 Mc/s) atmospheric radio noise data, NBS Technical Note No. 318 (U. S. Government Printing Office, Washington, D. C. 20402).

APPENDIX A

FORTRAN Computer Subroutine EVAL UT AN

```

SUBROUTINE EVAL UT AN
C LATITUDE (DLAT), LONGITUDE (DLON), AND THE NUMERICAL COEFFICIENTS (ABGD)
C ARE THE INPUT TO THIS EVALUATION ROUTINE. ATMOSPHERIC NOISE (ATN) IN
C UNIVERSAL TIME (NH) IS THE OUTPUT. HOURS 01 THROUGH 24 UT CORRESPOND
C TO ATN(1) THROUGH ATN(24).
COMMON /A/ DLON, DLAT, ABGD(21, 10, 5), ATN(24), NTO, NTE, NTS
DIMENSION C(10), S(10), TL(21, 5), TIME(5)
DATA (DR = 0.017453292520)
GLAT = DR * DLAT
GSIN = SIN(GLAT)
GCOS = COS(GLAT)
C NOTE PHASE SHIFT OF -2.14285714286 DEGREES.
RLON = DR * (DLON - 2.14285714286)
C EVALUATES THE GK FUNCTION (LATITUDE ANALYSIS).
DO 12 I = 1, 5
GKCS = 1.0
DO 12 J = 1, 21
G = 0.0
IF ((2 * (J / 2) - J) .EQ. 0) GKCS = GKCS * GCOS
MG = 10
IF (J .GE. 16) MG = 7
DO 20 K = 1, MG
KK = MG + 1 - K
20 IF ((KK - 1) .NE. 0) G = (G + ABGD(J, KK, I)) * GSIN
12 TL(J, I) = (G + ABGD(J, 1, I)) * GKCS
C EVALUATES LONGITUDINAL FOURIER COEFFICIENTS.
C(1) = COS(RLON)
S(1) = SIN(RLON)
DO 30 JJ = 2, 10
C(JJ) = C(1) * C(JJ - 1) - S(1) * S(JJ - 1)
30 S(JJ) = C(1) * S(JJ - 1) + S(1) * C(JJ - 1)
DO 32 I = 1, 5
F = TL(1, I)
DO 34 JL = 1, 10
34 F = F + TL(2 * JL, I) * S(JL) + TL(2 * JL + 1, I) * C(JL)
32 TIME(I) = F
C EVALUATES THE FOURIER COEFFICIENTS REPRESENTING THE DIURNAL VARIATION.
C TIME PHASE SHIFT (HOUR ANGLE IS PHASE SHIFTED -180. DEGREES).
DO 40 NH = NTO, NTE, NTS
NNH = NH
IF (NH .GT. 24) NNH = NH - 24
RHR = DR * (NNH * 15.0 - 180.0)
C(1) = COS(RHR)
S(1) = SIN(RHR)
C(2) = COS(RHR + RHR)
S(2) = SIN(RHR + RHR)
T = TIME(1)
DO 42 IT = 1, 2
42 T = T + TIME(2 * IT) * S(IT) + TIME(2 * IT + 1) * C(IT)
40 ATN(NNH) = T
RETURN
END

```